BB

Lund-MPh-97/11

Quadrupole Strength Function and Core Polarization in Drip Line Nuclei

I. Hamamoto, H. Sagawa and X. Z. Zhang

LUND INSTITUTE OF TECHNOLOGY

Department of Mathematical Physics

August 1997

Quadrupole Strength Function and Core Polarization in Drip Line Nuclei

I.Hamamoto[a], H.Sagawa[b] and X.Z.Zhang[a,c]

[a] Department of Mathematical Physics

Lund Institute of Technology at University of Lund

Lund, Sweden.

[b] Center for Mathematical Sciences, University of Aizu

Ikki-machi, Aizu-Wakamatsu

Fukushima 965, Japan.

[c] Institute of Atomic Energy, Beijing

The People's Republic of China.

ABSTRACT : Using the self-consistent Hartree-Fock calculation plus RPA with Skyrme interactions, the RPA quadrupole strength function is estimated in the coordinate space, including simultaneously both the isoscalar and the isovector correlation. We discuss the result of the isoscalar, the isovector and the electric quadrupole polarization of the Ca-isotopes from the proton drip line towards the neutron drip line. We study also the comparison of the polarizations in the $A=48$ mirror nuclei, ${}^{48}_{28}Ni_{20}$ and ${}^{48}_{20}Ca_{28}$, and the dependence of the polarizations of ${}^{28}_{8}O_{20}$ on various Skyrme interactions.

PACS numbers : 21.10.Re, 21.60.Jz, 23.20.Js

1 Introduction

The dynamics of nuclei far from the β-stability line can be studied by various interesting phenomena, which originate from smaller one-particle binding energies as well as the unusual ratio of the neutron number to the proton number. In ref.[1-4] it is pointed out that a large amount of multipole transition strength may appear in the very low-energy region just above the particle threshold. The nuclei need not be halo nuclei, but small angular momenta of particles should be possible in combination with hole orbitals with small binding energies. If no one-particle resonant states with the required quantum numbers are available for the excitation of particles from a given hole orbitals, the threshold strength consumes the major part of the transition strength. Thus, after taking into account the random phase approximation (RPA) correlation, the distribution of the whole response strength including giant resonances can be drastically changed compared with the case of β-stable nuclei.

In order to obtain an appreciable amount of the threshold strength in proton drip line nuclei, the proton number must be small, since the presence of a large Coulomb barrier hinders the occurrence of the phenomena uniquely connected with small binding energies of protons. On the other hand, proton drip line nuclei are relatively easy to reach experimentally and, thus, can be used for testing our understanding of the structure of nuclei far from β-stability, for example, the validity of both microscopic models and effective interactions.

From our knowledge [5] of β-stable nuclei the core polarization may be expected to be larger when a strong transition strength appears in the lower excitation-energy region of the core. The expectation is based on the fact that the static polarizability due to collective modes is inversely proportional to the frequencies of the collective modes. Thus, one might expect that the core polarizaton would be large when a large threshold strength appears in the very low-energy region of some drip line nuclei. It is shown in ref.[2] that the expectation is not really correct in the case of the neutron drip line nucleus, $^{28}_{8}O_{20}$.

Using the improved model in the present paper we examine more systematically the polarizability of nuclei far from β-stability line compared with β-stable nuclei.

As a microscopic model we first perform the spherical Hartree-Fock (HF) calculation with the Skyrme interactions and, then, use the RPA, which is solved in the coordinate space with the Green's function method [6,7]. In our previous publications except the most recent one [3] we made an approximation that the isovector (isoscalar) correlation was not taken into account while estimating the isoscalar (isovector) strength. To our knowledge, this approximation was made in all available publications, where the RPA equation was solved self-consistently in the coordinate space including the momentum-dependent terms t_1 and t_2 of the Skyrme interactions [7,8]. The approximation is almost exact for $Z=N$ nuclei. However, in the presence of neutron (or proton) excess the validity of the approximation might be questioned. Indeed, in ref.[3] we have shown that the simultaneous inclusion of the isoscalar (IS) and the isovector (IV) correlation leads to an interesting correlation structure of giant quadrupole resonances (GQR).

In section 2 we summarize the model and the formulae, especially the details of the polarization calculation. Taking the three Ca-isotopes (Z=20), the proton drip line nucleus, ${}^{34}_{20}Ca_{14}$, the $Z=N$ nucleus, ${}^{40}_{20}Ca_{20}$, and the nucleus with a large neutron excess, ${}^{60}_{20}Ca_{40}$, in section 3 we illustrate the dynamical features of quadrupole response unique in drip line nuclei compared with β-stable nuclei. Moreover, we compare the electric quadrupole polarization charge estimated for those three Z=20 nuclei.

As an example of mirror nuclei, in section 4 we compare the quadrupole properties of the proton drip line nucleus, ${}^{48}_{28}Ni_{20}$, with those of the β-stable nucleus, ${}^{48}_{20}Ca_{28}$. In ref.[2] we examined the quadrupole polarizability of ${}^{48}_{28}Ni_{20}$, using the model, in which the IS and the IV correlation are not simultaneously taken into account in solving the RPA. Employing the present model with the simultaneous inclusion of the IS and IV correlation we can make a better comparison of the properties of the mirror nuclei, which among light nuclei have an unusually large neutron and proton excess, respectively. Using

a given Skyrme interaction, in those mirror nuclei we find an appreciable difference of the properties of the lowest-lying 2^+ state and those of the GQR as well as electric quadrupole polarizabilities.

In section 5 we present the numerical result of quadrupole polarization of the light neutron drip line nucleus, ${}^{28}_{8}O_{20}$, and discuss it in comparison with the result in ref.[2], in which the IS and IV correlation were not simultaneously taken into account.

In section 6 we present further discussions and give the conclusion.

2 Model and Formulae

Using the same Skyrme interactions, we first perform the HF calculation and, then, solve the RPA equation in the coordinate space with the Green's function method. We estimate the RPA strength function

$$S(E) \equiv \sum_n |< n \mid Q \mid 0 >|^2 \, \delta(E - E_n) = \frac{1}{\pi} Im\, Tr(Q^\dagger G_{RPA}(E)\, Q) \qquad (1)$$

where Q expresses one-body operators, which are written as

$$Q_\mu^{\lambda=2,\tau=0} = \sum_i r_i^2\, Y_{2\mu}(\hat{r}_i) \qquad \text{for isoscalar quadrupole strength,} \qquad (2)$$

$$Q_\mu^{\lambda=2,\tau=1} = \sum_i \tau_z\, r_i^2\, Y_{2\mu}(\hat{r}_i) \qquad \text{for isovector quadrupole strength} \qquad (3)$$

and

$$Q_\mu^{\lambda=2,el} = \sum_i \frac{1}{2}(1 - \tau_z)\, r_i^2\, Y_{2\mu}(\hat{r}_i) \qquad \text{for electric quadrupole strength.} \qquad (4)$$

The RPA strength below the threshold can be obtained from the residue at the pole of the real part of the RPA Green's function.

In order to estimate the polarization due to the core excitations by particles, we use a perturbation, as in the literature [2,5,9]. The IS and the IV polarizability and the electric effective charge for quadrupole transitions are defined as

$$\chi_{pol}^{IS} = \frac{< \tilde{j} \,\|\, Q^{\lambda=2,\tau=0} \,\|\, \tilde{i} >}{< j \,\|\, Q^{\lambda=2,\tau=0} \,\|\, i >} - 1 \quad , \qquad (5)$$

$$\chi_{pol}^{IV} = \frac{< \tilde{j} \| Q^{\lambda=2,\tau=1} \| \tilde{i} >}{< j \| Q^{\lambda=2,\tau=1} \| i >} - 1 \tag{6}$$

and

$$e_{eff}/e = \frac{< \tilde{j} \| Q^{\lambda=2,el} \| \tilde{i} >}{< j \| Q^{\lambda=2,\tau=0} \| i >} \quad , \tag{7}$$

respectively. The electric polarization charge is $e_{pol}^{n} = e_{eff}$ for neutrons, while $e_{pol}^{p} = e_{eff} - e$ for protons. In eqs.(5), (6) and (7) $|\tilde{i}>$ and $|\tilde{j}>$ ($|i>$ and $|j>$) express the perturbed (unperturbed) single-particle wave functions,

$$|\tilde{i}> = |i> + \sum_{j,\omega_\lambda} \frac{< (j \times \omega_\lambda) i \mid V_{pv} \mid i >}{\varepsilon_i - (\varepsilon_j + \omega_\lambda)} \mid (j \times \omega_\lambda) i > \tag{8}$$

where V_{pv} is the particle-vibration coupling interaction, which is constructed based on the same Skyrme interaction as the one used in both the HF and the RPA calculation [2,9]. The reduced transition matrix element for the one-body operator Q^λ is written as

$$< \tilde{j} \| Q^\lambda \| \tilde{i} > = < j \| Q^\lambda \| i > + \sum_{\omega_\lambda} \frac{2\omega_\lambda}{(\varepsilon_i - \varepsilon_j)^2 - \omega_\lambda^2} \frac{\sqrt{2i+1} < (j \times \omega_\lambda) i \mid V_{pv} \mid i >}{\sqrt{2\lambda+1}} < \omega_\lambda \| Q^\lambda \| 0 > . \tag{9}$$

In numerical examples of the present work we consider only the static polarizability and, thus, we have $\varepsilon_i = \varepsilon_j$ in (9). The particle-vibration coupling V_{pv} is derived in ref.[2,9] from the Skyrme interaction approximating the momentum derivative operators $\mathbf{k}$ and $\mathbf{k}'$ by the Fermi momentum k_F so that one can use directly the RPA transition densities for the calculation of the matrix element. This approximation was made only here in constructing the particle-vibration coupling. Then, we write

$$V_{pv}(\vec{r_1} - \vec{r_2}) = \delta(\vec{r_1} - \vec{r_2}) \left(V_{pv}^{\tau=0}(r) + (\vec{\tau_1} \cdot \vec{\tau_2}) V_{pv}^{\tau=1}(r) \right) \tag{10}$$

where

$$V_{pv}^{\tau=0}(r) = \{ \frac{3}{4} t_0 + \frac{3}{48}(\alpha+2)(\alpha+1) t_3 \rho^\alpha(r) + \frac{1}{8} k_F^2 [3t_1 + t_2(5+4x_2)] \}, \tag{11}$$

and

$$V_{pv}^{\tau=1}(r) = \{ -\frac{1}{4} t_0 (1+2x_0) - \frac{1}{24} t_3 (1+2x_3) \rho^\alpha(r) + \frac{1}{8} k_F^2 [-t_1(1+2x_1) + t_2(1+2x_2)] \}, \tag{12}$$

where $\boldsymbol{r} = \frac{1}{2}(\boldsymbol{r}_1 + \boldsymbol{r}_2)$. Then the coupling matrix is evaluated to be

$$< (j \times \omega_\lambda)i \mid V_{pv} \mid i > = \frac{1}{\sqrt{2i+1}} \int r^2 dr \, V_{pv}(r) \, \delta\rho(r) R_j(r) R_i(r) < j \parallel Y_\lambda \parallel i > \qquad (13)$$

where the radial transition density $\delta\rho(r)$ is defined by

$$\delta\rho(\vec{r}) \equiv \delta\rho(r) \, Y_{\lambda\,\mu}(\hat{r}) \qquad (14)$$

and $R(r)$ expresses the radial wave functions of single-particle states.

In the present paper we estimate the polarizabilities using two different methods, depending on the values of $\mid N-Z \mid$. In numerical examples we take nuclei with either $\mid N-Z \mid >> 1$ or $N=Z$. First, we consider the case of $\mid N-Z \mid >> 1$, in which the major part of the IV excitations have the same total isospin $T = \mid T_0 \mid$ (where $T_0 \equiv (N-Z)/2$) as that of the IS excitations. Thus, we do not explicitly use the isospin formalism, and the particle-vibration coupling V_{pv} includes both the IS and the IV part, irrespective of the IS or the IV or the electric character of the quadrupole operator Q^λ . This simultaneous incluson was not done in ref.[2]. We use

$$V_{pv}(r) \, \delta\rho(r) \; = \; V_{pv}^{\tau=0}(r) \, [\, \delta\rho_{IS}^n(r) + \delta\rho_{IS}^p(r) \,] \; + \; \tau_z^{particle} \, V_{pv}^{\tau=1}(r) \, [\, \delta\rho_{IV}^n(r) - \delta\rho_{IV}^p(r) \,] \qquad (15)$$

in the integrand on the r.h.s. of eq.(13), where $[\, \delta\rho_{IS}^n(r) + \delta\rho_{IS}^p(r) \,]$ and $[\, \delta\rho_{IV}^n(r) - \delta\rho_{IV}^p(r) \,]$ expresses the radial transition density of the core response to the external IS and the IV field in (2) and (3), respectively.

In the present continuum calculation the transition density at a given energy may be a superposition of contributions from many states with different dynamical structure. Thus, the neutron (proton) part of the IS transition density $\delta\rho_{IS}^n$ ($\delta\rho_{IS}^p$) at a given energy may not necessarily be the same as that of the IV transition density $\delta\rho_{IV}^n$ ($\delta\rho_{IV}^p$) at the same energy, in contrast to the case of an isolated quantum state. In the latter case the neutron (or proton) part of the quadrupole transition density is uniquely defined, irrespective of the response to the external IS or IV field, namely ; $\delta\rho_{IS}^n = \delta\rho_{IV}^n$ and $\delta\rho_{IS}^p = \delta\rho_{IV}^p$. In

our present model the transition density $[\delta\rho^n_{IS} + \delta\rho^p_{IS}]$ contributes to the core matrix-element $< \omega_\lambda \| Q^{\lambda=2,\tau=0} \| 0 >$ in (9) and $[\delta\rho^n_{IV} - \delta\rho^p_{IV}]$ to $< \omega_\lambda \| Q^{\lambda=2,\tau=1} \| 0 >$, while the transition density of the core response to the electric field, which may be different from either $\delta\rho^p_{IS}$ or $\delta\rho^p_{IV}$, is used in the calculation of $< \omega_\lambda \| Q^{\lambda=2,el} \| 0 >$.

In numerical examples we show the calculated electric polarization charges consisting of e^{IS}_{pol} and $\tau_z\, e^{IV}_{pol}$. The IS (IV) polarization charge e^{IS}_{pol} (e^{IV}_{pol}) expresses the contribution coming from the first (second) term containing $V^{\tau=0}_{pv}$ ($V^{\tau=1}_{pv}$) in the particle-vibration coupling (15). The total electric polarization charge is written as

$$e_{pol} = \begin{cases} e^n_{pol} = e^{IS}_{pol} + e^{IV}_{pol} & \text{for neutrons} \\ e^p_{pol} = e^{IS}_{pol} - e^{IV}_{pol} & \text{for protons} \end{cases} \tag{16}$$

For the electric polarization charges of protons and neutrons in drip line nuclei with $|N-Z| >> 1$, the relation such as

$$e^{IS}_{pol} = \frac{Z}{A}\, \chi^{IS}_{pol} \tag{17}$$

does not work, though we should have the relation

$$e_{pol} = \frac{1}{2}\, (\chi^{IS}_{pol} - \tau_z\, \chi^{IV}_{pol}) \tag{18}$$

within the accuracy of the numerical method used in the present work. The quantities, χ^{IS}_{pol} and χ^{IV}_{pol} , express the mass and the IV quadrupole polarizabilities, which may be measured experimentally. We note that χ^{IS}_{pol} and χ^{IV}_{pol} , which are defined in eqs.(5) and (6), depend explicitly on τ_z since both the IS and the IV part of the particle-vibration coupling are simultaneously taken into account, as is expressed in eq.(15).

For the mode corresponding to oscillations of neutrons with respect to protons in the case of $|N-Z| >> 1$, it may be of physical interests to consider a field that acts on the difference of the isospin from its mean value. Defining the field operator (see, for example, eq.(6-385) of ref.[5])

$$F^{\lambda=2,\tau=1}_{\mu} = \sum_i (\tau_z - \frac{N-Z}{A})\, r_i^2\, Y_{2\mu}(\hat{r}_i) \quad , \tag{19}$$

we estimate the corresponding effective IV polarizability

$$k_{pol}^{eff}(IV) \;=\; \tau_z\,\chi_{pol}^{IV} \;-\; \frac{N-Z}{A}\,\chi_{pol}^{IS} \qquad . \tag{20}$$

We note that the expression (20) as the effective IV polarizability in response to the field in (19) is obtained as the result of the simultaneous inclusion of the IS and the IV interaction in the particle-vibration coupling in (15). Later in numerical examples we tabulate calculated values of χ_{pol}^{IS} and $k_{pol}^{eff}(IV)$, which may be of physical interests, besides the electric polarization charge.

Next, in the case of $N=Z$ the isospin (=0 and 1) of the IS and the IV excitations is a pretty good quantum number of the total system. Then, those two kinds of excitations have to be treated separately keeping the isospin as a good quantum number. Instead of eq.(15) we use

$$V_{pv}(r)\,\delta\rho(r) \;=\; V_{pv}^{\tau=0}(r)\,[\,\delta\rho_{IS}^{n}(r)+\delta\rho_{IS}^{p}(r)\,] \qquad \text{for isoscalar quadrupole polarization} \tag{21}$$

and

$$V_{pv}(r)\,\delta\rho(r) \;=\; V_{pv}^{\tau=1}(r)\,[\,\delta\rho_{IV}^{n}(r)-\delta\rho_{IV}^{p}(r)\,] \qquad \text{for isovector quadrupole polarization} \tag{22}$$

in the integrand on the r.h.s. of eq.(13). In the IS polarization the transition density $[\,\delta\rho_{IS}^{n}+\delta\rho_{IS}^{p}\,]$ is used for the core matrix-element $<\omega_\lambda\|Q^{\lambda=2,\tau=0}\|0>$ in (9), while in the IV polarization $[\,\delta\rho_{IV}^{n}-\delta\rho_{IV}^{p}\,]$ is employed in the estimate of $<\omega_\lambda\|Q^{\lambda=2,\tau=1}\|0>$. The electric polarization receives a contribution both from the IS core-excitations with $V_{pv}(r)\,\delta\rho(r)$ in (21) and the transition density $\delta\rho_{IS}^{p}$ in $<\omega_\lambda\|Q^{\lambda=2,el}\|0>$, and from the IV excitations with $V_{pv}(r)\,\delta\rho(r)$ in (22) and $\delta\rho_{IV}^{p}$ in $<\omega_\lambda\|Q^{\lambda=2,el}\|0>$.

3 Quadrupole Strength and Polarization Charge of Ca-isotopes

In the upper (lower) part of figs.1a-1c we show the calculated IS (IV) RPA quadrupole strength compared with the strength estimated with the T=0 (T=1) correlation only, for

the nuclei, ${}^{34}_{20}Ca_{14}$, ${}^{40}_{20}Ca_{20}$ and ${}^{60}_{20}Ca_{40}$. For ${}^{34}_{20}Ca_{14}$ there are two very sharp 2^+ states (at 3.17 and 7.56 MeV) drawn by the solid line, which originate from $0\hbar\omega_0$ excitations of neutrons. The physics extracted from the comparison between the solid line and the dotted line in figs.1a-1c is exactly the same as the one already discussed in ref.[3]. As seen from the upper part of the figs.1a and 1c, the IS GQR peak energy shifts from 16.74 to 17.45 MeV for ${}^{34}_{20}Ca_{14}$ and from 13.71 to 14.80 MeV for ${}^{60}_{20}Ca_{40}$, due to the inclusion of the IV (T=1) correlation in the presence of the proton and the neutron excess, respectively. The magnitude of the shift in the neutron-rich nucleus ${}^{60}Ca$, 14.80−13.71=1.09 MeV, is obtained almost exactly by scaling the calculated shifts in ${}^{28}_{8}O_{20}$, ${}^{48}_{20}Ca_{28}$ and ${}^{70}_{20}Ca_{50}$ with the quantity $((N-Z)/A)^2A^{-1/3}$, as was already discussed for the nuclei with neutron excess in ref.[3].

In fig.2 we plot the RPA electric quadrupole strength for the neutron drip line nucleus, ${}^{60}_{20}Ca_{40}$, a β-stable nucleus, ${}^{40}_{20}Ca_{20}$, and the proton drip line nucleus, ${}^{34}_{20}Ca_{14}$. The peaks at $14< E <18$ MeV express the IS GQR, while the strength for $E>20$ MeV denotes the IV GQR. A low-lying proton strength hardly appears in the RPA solution for the neutron drip line nucleus ${}^{60}Ca$, while the neutron threshold strength gives a significant amount of the IS and the IV strength in the low energy region of $E_x < 13$ MeV, as seen in fig.1(c). In the region of IV GQR the nucleus ${}^{60}Ca$, which has a large neutron excess, has the largest proton strength, while ${}^{34}Ca$ has the smallest proton strength. This is because even in the presence of the proton or the neutron excess the IV GQR tends to have a rather pure isovector character [3,5] with very little isoscalar moment. As a result of it, in ${}^{60}Ca$ a smaller proton strength is available for the IS GQR. Among the three Z=20 isotopes the sharpest concentration of the proton strength in IS GQR is observed in ${}^{40}Ca$. In ${}^{34}Ca$ the low-lying proton threshold strength (namely, the low-energy tail of the dashed line seen in fig.2) is clearly seen and takes some of the proton strength.

Using the SkM* interaction, in tables 1(a)-1(c) we show some calculated static polarizabilities of the IS, the IV and the electric quadrupole operator for ${}^{40}Ca$, ${}^{60}Ca$ and ${}^{34}Ca$

, respectively. Since the nucleus ^{34}Ca is not an ℓ-s closed shell nucleus, we obtain the two low-lying 2^+ states at 3.17 and 7.56 MeV, which make considerable contributions to the total quadrupole polarizabilities due to the low energies, in spite of the fact that those states are not very collective. The energies as well as the collectivity of those low-lying 2^+ states are sensitive to the energy difference between the two neutron orbitals, $1d_{5/2}$ and $2s_{1/2}$, and, thus, may depend appreciably on the Skyrme interactions used. Consequently, without having any experimental informations on the energy difference the accuracy of the calculated contributions from the low-lying 2^+ states to the polarizabilities is difficult to be estimated. In table 1(c) the polarizabilities excluding those two contributions are also shown in parentheses, for reference.

For the nucleus ^{40}Ca the relation between the IS, IV and electric polarizabilities, eqs.(17) and (18), works well. Furthermore, the calculated values of the IS polarizability are in remarkable agreement with those obtained by using the harmonic oscillator model [5]. We have checked that for this ℓ-s closed shell nucleus the values estimated by using the SG2 interaction instead of SkM* interaction are almost the same as those tabulated in table 1(a). The averaged value of the socalled empirical IS effective charge in the mass region $A = 20 - 36$, which are obtained [10] by comparing the full multiparticle $(0d\,1s)^n$ wave functions with the experimental E2 matrix elements, is $(0.35 \pm 0.05)\,e$, compared with our value, $0.51\,e$. As to the IV polarizability, our calculated values are only about a half of those given by the oscillator model [5], consistent with the fact that our averaged calculated frequency of the IV GQR is systematically lower than the one given in the model of ref.[5]. The frequency of the IV GQR is not yet experimentally established, and in the harmonic oscillator model of ref.[5] the interaction strength in the IV channel is known to reproduce the measured frequencies of the IV giant dipole resonance. The self-consistent HF plus RPA with the SkM* interaction gives also a good description of the IV giant dipole resonance, because of the combined effect of the weak IV interaction with the small effective mass.

As seen from tables 1(b) and 1(c), both in neutron rich nucleus ${}^{60}_{20}Ca_{40}$ and in the proton drip line nucleus ${}^{34}_{20}Ca_{14}$ the calculated values of e^{IS}_{pol} and e^{IV}_{pol} are not very different for neutrons and protons. The small difference comes from the difference between the one-particle wave functions of neutrons and protons, since in ${}^{60}_{20}Ca_{40}$ (${}^{34}_{20}Ca_{14}$) protons (neutrons) are much more bound than neutrons (protons). The proton threshold strength below 10 MeV (see fig.2) in ${}^{34}Ca$ makes very small contributions to the polarization charge with an opposite sign to those of the IS GQR (and the states at 3.17 and 7.56 MeV), due to the unique form factor which was explained in ref.[2] for the similar threshold strength in ${}^{28}_{8}O_{20}$. In ${}^{60}_{20}Ca_{40}$ the considerable RPA threshold strength below 10 MeV (see Fig.1(c)) hardly carries the proton strength and, thus, contributes little to the polarization charge. Therefore, the essential part of the calculated polarization charge comes from the IS GQR and the IV GQR. If we literally apply the formula, eq.(6-386b) in ref.[5],

$$e_{pol} = e\left(\frac{Z}{A} - 0.32\,\frac{N-Z}{A} + (0.32 - 0.3\,\frac{N-Z}{A})\,\tau_z\right) \tag{23}$$

to the present Ca-isotopes, we obtain

$$e_{pol} = e(0.22 + 0.22\,\tau_z) \qquad \text{for } {}^{60}_{20}Ca_{40} \tag{24}$$

and

$$e_{pol} = e(0.65 + 0.37\,\tau_z) \qquad \text{for } {}^{34}_{20}Ca_{14} \quad . \tag{25}$$

The expression (23) is derived using the harmonic oscillator model and contains the contributions only from the IS GQR and the IV GQR. The e^{IS}_{pol} values in ${}^{60}Ca$ in table 1(b), $0.25\,e$ for neutrons and $(0.28\text{-}0.30)\,e$ for protons, are appreciably larger than $0.22\,e$ in (24). The largeness is a feature of very neutron-rich nuclei near the neutron drip line, since the property of the IS GQR in such nuclei is considerably influenced [3] by the large neutron excess together with the presence of the threshold strength. In contrast, the e^{IS}_{pol} values coming from the IS GQR in the proton drip line nucleus ${}^{34}Ca$, $0.55\,e$ for neutrons and $(0.48\text{-}0.54)\,e$ for protons shown in the parenthesis of table 1(c), are smaller than $0.65\,e$ in (25). The e^{IV}_{pol} values in table 1(b) for ${}^{60}Ca$, $0.07\,e$ for neutrons and

$0.11\,e$ for protons, are much smaller than $0.22\,e$ in (24), while in table 1(c) for ^{34}Ca we have $0.19\,e$ for both neutrons and protons compared with $0.37\,e$ in (25). Thus, in both ^{60}Ca and ^{34}Ca the e^n_{pol} values are much closer to the e^p_{pol} values than expected from the expressions (24) and (25).

In the $N=Z$ nucleus ^{40}Ca the polarizability $k^{eff}_{pol}(IV)$ is equal to $\tau_z\chi^{IV}_{pol}$. For $N\neq Z$ nuclei the effective polarizability $k^{eff}_{pol}(IV)$ plays the role of $\tau_z\chi^{IV}_{pol}$ in $N=Z$ nuclei. In ^{60}Ca both χ^{IS}_{pol} and $\mid k^{eff}_{pol}(IV)\mid$ values for protons are larger than those for neutrons, due to the large neutron excess. In contrast, as to the contributions from the GQR in ^{34}Ca shown inside the parentheses of table 1(c), due to the proton excess both χ^{IS}_{pol} and $\mid k^{eff}_{pol}(IV)\mid$ values for neutrons are larger than those for protons. It is interesting to note that we obtain very small total values ($= 0.02$) of $k^{eff}_{pol}(IV)$ for neutrons in ^{34}Ca, namely the effective IV operator for neutrons receives no polarization effect.

4 Comparison of Two Mirror Nuclei, $^{48}_{28}Ni_{20}$ and $^{48}_{20}Ca_{28}$

In ref.[2] we have studied the quadrupole properties of $^{48}_{28}Ni_{20}$ and presented some discussion in comparison with those of $^{48}_{20}Ca_{28}$. In the approximation used in ref.[2] the estimated excitation energy of the lowest-lying 2^+ state in $^{48}_{20}Ca_{28}$ was 3.0, 3.0 and 4.0 MeV for the SkM*, SG2 and SIII interaction, respectively. Including simultaneously both the IS and the IV part of the Skyrme interaction in the RPA of the present model the estimated energy is shifted to 3.6, 3.6 and 4.6 MeV for the SkM*, SG2 and SIII interaction, respectively. The estimatedd energy of the lowest 2^+ state is sensitive to the energy difference between the $1f_{7/2}$ and the $2p_{3/2}$ orbitals. Since the observed energy of the lowest 2^+ state in $^{48}_{20}Ca_{28}$ is 3.83 MeV, it seems to be reasonable to use the SkM* (or SG2) interaction in the present model calculations of those A=48 nuclei.

The calculated binding energy of the $1d_{3/2}$ neutrons (protons) in ^{48}Ni (^{48}Ca) is 21.60 (14.70) MeV, while that of the $1f_{7/2}$ protons (neutrons) in ^{48}Ni (^{48}Ca) is 1.34 (10.42) MeV. Despite of these large binding energy differences there is not much difference of

the mean square radius of neutrons (protons), 3.42 fm (3.70 fm), in the ground state of $^{48}_{28}Ni_{20}$ from that of protons (neutrons), 3.45 fm (3.60 fm) , in $^{48}_{20}Ca_{28}$, due to the presence of the Coulomb barrier. Thus, one may expect that the two nuclei are pretty good mirror nuclei, as far as the properties of the ground states are concerned. However, the dynamical properties can be considerably different in the two nuclei, as will be seen in the following. In figs.3a-3d we show the comparison between various quadrupole response functions of the mirror nuclei, $^{48}_{28}Ni_{20}$ and $^{48}_{20}Ca_{28}$, calculated with the SkM* interaction. The strength of the two low-lying 2^+ states calculated at 3.59 and 9.00 MeV in $^{48}_{20}Ca_{28}$ are not plotted in the figures, since those states lie below the particle threshold and, thus, have no width in the present calculation.

In fig.3a the RPA IS strength of the two mirror nuclei is compared. The proton p-h excitation energy of $1f_{7/2} \rightarrow 2p_{3/2}$ in ^{48}Ni is 3.33 MeV, which is 15 percent smaller than the corresponding neutron p-h excitation energy in ^{48}Ca , 3.86 MeV. This smaller unpertrubed p-h excitation energy leads to the lower excitaton energy of the lowest RPA 2^+ state in ^{48}Ni , 3.02 MeV, than that in ^{48}Ca , 3.59 MeV. It is seen that the peak energy of the IS GQR in ^{48}Ni , 16.01 MeV (which was 15.47 MeV without including the T=1 correlation), is also lower than the one in ^{48}Ca , 16.63 MeV (16.33 MeV without the T=1 correlation). Since the total mean square radius is not really different in the two nuclei, the energy weighted sum rule (EWSR) for the IS quadrupole strength is nearly the same.

In fig.3b the RPA IV strength is compared. We hardly find any qualitative difference in the properties of the IV GQR lying at $E_x > 20$ MeV in the two mirror nuclei, though the IV strength contained in the IS GQR, of which the peak energy is 16.01 and 16.63 MeV for ^{48}Ni and ^{48}Ca , respectively, is appreciably different. In figs.3c and 3d we compare the mirror strength, $Z = N$ =28 and $N = Z$ =20 in the two nuclei. It is seen that in the IS GQR the proton strength in $^{48}_{28}Ni_{20}$ is much larger than the neutron strength in $^{48}_{20}Ca_{28}$, while no significant difference can be seen in the IV GQR region.

In tables 2(a)-2(b) we tabulate the calculated static polarizabilities of the IS, the IV

and the electric quadrupole operator for $^{48}_{28}Ni_{20}$ and $^{48}_{20}Ca_{28}$. For reference, inside of the parentheses the polarizabilities are shown, which are calculated by excluding the contributions of the two low-lying peaks that originate from the excitations of the $1f_{7/2}$ nucleons. The two low-lying peaks of $^{48}_{28}Ni_{20}$ for E <9 MeV consist predominantly of proton configurations, while the two low-lying 2^+ states of $^{48}_{20}Ca_{28}$ at 3.59 and 9.00 MeV consist mainly of neutron configurations. Those low-lying RPA states contribute appreciably to the polarizabilities as seen in tables 2(a) and 2(b), though they are not very collective. Comparing the calculated e_{pol} values of table 2(a) with those of table 2(b), we find that e^{IS}_{pol} values in ^{48}Ni are about twice of those in ^{48}Ca while e^{IV}_{pol} values in ^{48}Ni are by an order of magnitude larger than those in ^{48}Ca . Since $e^{n}_{pol} = e^{IS}_{pol}+e^{IV}_{pol}$ and $e^{p}_{pol} = e^{IS}_{pol}-e^{IV}_{pol}$, the e^{p}_{pol} values in ^{48}Ni is comparable with the e^{n}_{pol} values in ^{48}Ca , while the e^{n}_{pol} values in ^{48}Ni is about a factor of 3 larger than e^{p}_{pol} values in ^{48}Ca .

We find that for the $1d_{3/2}$ and the $1f_{7/2}$ orbitals the calculated χ^{IS}_{pol} values of neutrons (protons) in ^{48}Ni are remarkably similar to those of protons (neutrons) in ^{48}Ca . The similarity shows that the notion of mirror nuclei works for the quantity. It would be very interesting to see experimentally the difference of $k^{eff}_{pol}(IV)$ values between neutrons and protons, namely, to see whether or not in ^{48}Ni (^{48}Ca) the effective IV operator for protons (neutrons) is not reduced while that for neutrons (protons) is strongly reduced.

Because of the relatively large value of $\frac{|N-Z|}{A} = \frac{8}{48} = 0.17$, the properties of the low-lying 2^+ states are considerably changed when the IS and the IV correlation is simultaneously taken into account. Thus, we have found that the IS polarization charge estimated for ^{48}Ni in ref.[2] was much larger than the one in the present calculations, while the IV polarization charge was smaller.

5 Quadrupole properties of $^{28}_{8}O_{20}$

In the upper (lower) part of figs.4a-4c we show the calculated IS (IV) RPA quadrupole strength of the neutron drip line nucleus, $^{28}_{8}O_{20}$, using the SkM*, SG2 and SIII interac-

tions. The strength function with the SG2 interaction is previously calculated in ref.[4], treating the continuum by expanding wave functions in terms of harmonic oscillator bases. The comparison between the solid and the dotted line in fig.4 exhibits the importance of the simultaneous inclusion of the T=0 and the T=1 correlation in the calculation of the nuclei with $|N-Z|>>1$. In ref.[3] the RPA strength estimated by using the SkM* interaction is shown together with radial transition densities of the GQR. On the other hand, in ref.[2] the electric polarization charges are presented, which are estimated by using the approximation in which the IV (IS) RPA correlation was not taken into account while calculating the IS (IV) strength. For completeness, we include fig.4a, which is taken partly from ref.[3]. Since the particle (namely, neutron) threshold depends appreciably on the Skyrme interactions (1.79, 3.25 and 1.11 MeV for the SkM*, SG2 and SIII interaction, respectively), the separation of the low-energy threshold strength from the IS GQR peak depends on the Skyrme interactions used. The energy of the IS GQR is nearly the same for the three Skyrme interactions, while the IV GQR for the SIII interaction lies somewhat higher than that for the SkM* and the SG2 interaction, which may be due to a larger symmetry energy coefficient of the SIII interaction.

In tables 3(a)-3(b) we compare the calculated static polarizabilities of the IS, the IV and the electric quadrupole operator, which are obtained by using the SkM* and the SIII interaction. The polarization charge of the neutrons in the $1d_{3/2}$ orbital is clearly small, since the binding energy of the neutrons is so small that the neutrons are not efficient in polarizing the core. The electric polarization charge in table 3 may be compared with the one in (23) obtained from the harmonic oscillator model,

$$e_{pol} \;=\; e\,(0.15 + 0.19\,\tau_z) \qquad \text{for } {}^{28}_{8}O_{20} \qquad . \tag{26}$$

The proton polarization charge obtained literally from eq.(26) is $-0.04\,e$, in which the contribution from the IV part overcancels that from the IS part. However, as seen already in sect.3 for another very neutron-rich nucleus ${}^{60}_{20}Ca_{40}$, except for the $1d_{3/2}$ neutrons the e^{IS}_{pol} values of ${}^{28}_{8}O_{20}$ in table 3 are (50-70) percent larger than $0.15\,e$ given in (26),

while the e_{pol}^{IV} values are a factor 2-3 smaller than $0.19\,e$ in (26). Thus, calculated e_{pol} values for protons remain to be positive, $(0.15\text{-}0.17)\,e$, depending slightly on Skyrme interactions. The analysis of the contribution from the low-lying threshold strength to the quadrupole polarization charges in ^{28}O , which is described in ref.[2], remains valid. However, the approximation used in ref.[2], in which the IV (IS) correlation was not taken into account while estimating the IS (IV) strength, has turned out to be rather poor for very neutron-rich nuclei. Thus, the quantitative values of e_{pol} are changed compared with those in ref.[2].

6 Conclusion and Discussions

Using the self-consistent Hartree-Fock calculation plus RPA with Skyrme interactions, the RPA quadrupole strength function is estimated in the coordinate space, including simultaneously both the IS and the IV correlation. In $N >> Z$ ($N << Z$) nuclei the calculated IS GQR carries also an appreciable amount of the IV density due to the neutron (proton) excess, while the calculated IV GQR carries very little IS density. In neutron drip line nuclei the averaged frequency of the calculated IS GQR tends to be lower than the systematics in β-stable nuclei. In neutron-rich nuclei ^{60}Ca and ^{28}O the large neutron quadrupole strength appears just above the threshold, while the proton threshold strength is seen below the IS GQR in the proton drip line nucleus ^{34}Ca .

Using the particle-vibration coupling model based on the RPA solutions, we have estimated electric polarization charges as well as the IS and the IV polarizability. It is clearly seen that the polarizabilities are small for nucleons with small binding energies and small orbital angular momenta, since those nucleons do not polarize the core nuclei efficiently. In nuclei with $|N-Z| >> 1$ the effective IV polarizability $k_{pol}^{eff}(IV)$, defined in (20), is of more physical interests than $\tau_z \chi_{pol}^{IV}$. The contribution from the GQR to $k_{pol}^{eff}(IV)$ is negative (positive) for neutrons (protons). Our estimated values of $k_{pol}^{eff}(IV)$ are almost vanishing for neutrons in ^{34}Ca and ^{48}Ca , while they are as large

as 0.7 for protons in those nuclei. Since the excitations of the IV modes by nucleons may be governed by a factor of $(1 + \tau_z k_{pol}^{eff}(IV))^2$, it would be interesting to check experimentally whether or not neutrons can excite the IV modes of those nuclei much more efficiently than protons. Our calculated values of e_{pol}^{IV} are considerably smaller than those given by the oscillator model of ref.[5], since the IV strength of Skyrme interactions are clearly weaker than the corresponding strength in the model of ref.[5].

In β-stable $N = Z$ nucleus $^{40}_{20}Ca_{20}$ the estimated IS polarization is almost equal to the one given by the harmonic oscillator model in [5], while the calculated IV polarization is much smaller than that in [5]. In drip line nuclei the low-lying threshold strength contributes, in general, little to the polarizability and, thus, the quadrupole polarizability of the ℓ-s closed nuclei is in essence determined by the properties of the IS and the IV quadrupole giant resonance. In neutron drip line nuclei such as $^{60}_{20}Ca_{40}$ and $^{28}_{8}O_{20}$ the IS polarization is appreciably larger than the values estimated in the oscillator model. In contrast, in proton drip line nuclei, $^{34}_{20}Ca_{14}$ and $^{48}_{28}Ni_{20}$, the IS polarization coming from the GQR is slightly smaller than the values given by the oscillator model calculation.

The ground state properties of the mirror nuclei, $^{48}_{28}Ni_{20}$ and $^{48}_{20}Ca_{28}$, are very similar, in spite of the large difference in the fermi levels of respective mirror nucleons ; $N = 20$ vs. $Z = 20$, and $Z = 28$ vs. $N = 28$. However, the dynamical properties, such as the excitation spectra and the polarization charges, of those two nuclei are found to be considerably different.

In $^{28}_{8}O_{20}$ the calculated threshold energy depends appreciably on the Skyrme interactions used and, thus, the degree of the separation of the IS GQR from the low-energy threshold strength depends on Skyrme interactions. On the other hand, the calculated polarization charges are relatively insensitive to the Skyrme interactions used, since the essential contributions to the polarizability come from the GQR, of which the properties are nearly the same for all reasonable Skyrme interactions. The polarizability of neutrons in the $1d_{3/2}$ orbital is always much smaller than that in the $1d_{5/2}$ orbital, because the $1d_{3/2}$

neutrons cannot polarize the core nucleus efficiently due to the small binding energy.

One of the authors (X.Z.Z.) acknowledges the financial support provided by the Wenner-Gren Foundation, which makes him possible to work at the Lund Institute of Technology.

References

[1] I.Hamamoto, H.Sagawa and X.Z.Zhang, Phys.Rev. **C53** (1996) 765.

[2] I.Hamamoto and H.Sagawa, Phys.Rev. **C53** (1996) R1492 ; Phys.Rev. **C 54** (1996) 2369 ; Phys.Lett.**B394** (1997) 1.

[3] I.Hamamoto, H.Sagawa and X.Z.Zhang, Phys.Rev. **C55** (1997) 2361.

[4] F.Catara, E.G.Lanza, M.A.Nagarajan and A.Vitturi, Nucl.Phys., **A614** (1997) 86.

[5] A.Bohr and B.R.Mottelson, Nuclear Structure, Vol.II (Benjamin, Reading. MA, 1975).

[6] S.Shlomo and G.F.Bertsch, Nucl.Phys.**A243** (1975) 507.

[7] N.Van Giai and H.Sagawa, Nucl.Phys. **A371** (1981) 1.

[8] K.F.Liu and G.E.Brown, Nucl.Phys. **A265** (1976) 385.

[9] H.Sagawa and B.A.Brown, Nucl.Phys. **A430** (1984) 84.

[10] B.A.Brown, R.Radhi and B.H.Wildenthal, Phys.Reports, **101** (1983) 313.

Figure captions

Figure 1 : The RPA quadrupole strength function of Ca-isotopes, which is calculated using the SkM* interaction ; (a) the proton drip line nucleus $^{34}_{20}Ca_{14}$, (b) the β-stable $N=Z$ nucleus $^{40}_{20}Ca_{20}$, and (c) the very neutron-rich nucleus $^{60}_{20}Ca_{40}$, as a function of excitation energy. The upper part : the isoscalar RPA quadrupole strength with (solid lines) and without (dotted lines) the isovector ($T=1$) correlation. The lower part : the isovector RPA quadrupole strength with (solid lines) and without (dotted lines) the isoscalar ($T=0$) correlation. In the case of $^{34}_{20}Ca_{14}$ there are two very sharp low-lying 2^+ states at 3.17 and 7.56 MeV (expressed by solid lines) superposed on the gradually increasing proton threshold strength.

Figure 2 : The RPA quadrupole response for protons in the three Ca-isotopes. The peaks at $14<E<18$ MeV express the IS GQR, while the strength for $E>20$ MeV denotes the IV GQR. In our present method the spreading width of the collective modes is not included, though a proper strength function in the continuum is obtained.

Figure 3 : Comparison between various RPA quadrupole strength functions of the mirror nuclei, $^{48}_{28}Ni_{20}$ and $^{48}_{20}Ca_{28}$, which are calculated with the SkM* interaction. The strengths of two low-lying 2^+ states calculated at 3.59 and 9.00 MeV in $^{48}_{20}Ca_{28}$ are not plotted in the figures, since the widths of those states are vanishing. (a) The RPA isoscalar strength ; (b) The RPA isovector strength ; (c) The RPA response strength of the proton (neutron) quadrupole operator in $^{48}_{28}Ni_{20}$ ($^{48}_{20}Ca_{28}$) : (d) The RPA response strength for the neutron (proton) quadrupole operator in $^{48}_{28}Ni_{20}$ ($^{48}_{20}Ca_{28}$).

Figure 4 : The RPA quadrupole strength functions of the neutron drip line nucleus $^{28}_{8}O_{20}$, which are calculated using three kinds of the standard Skyrme interactions : (a) the SkM* interaction, (b) the SG2 interaction, and (c) the SIII interaction. The upper part : Comparison between the isoscalar RPA strength with and without the

isovector ($T = 1$) correlation. The lower part : Comparison between the isovector RPA strength with and without the isoscalar ($T = 0$) correlation. Fig.4a is taken from ref.[3].

$^{40}_{20}Ca_{20}$		neutrons					protons				
f	i	χ^{IS}_{pol}	$k^{eff}_{pol}(IV)$	e^{IS}_{pol}	$\tau_z\, e^{IV}_{pol}$	e^{n}_{pol}	χ^{IS}_{pol}	$k^{eff}_{pol}(IV)$	e^{IS}_{pol}	$\tau_z\, e^{IV}_{pol}$	e^{p}_{pol}
$1d_{5/2}$	$1d_{5/2}$	0.97	-0.30	0.53	0.15	0.68	0.97	0.30	0.52	-0.15	0.37
$1d_{3/2}$	$1d_{3/2}$	0.94	-0.29	0.51	0.14	0.65	0.93	0.28	0.50	-0.14	0.36
$1f_{7/2}$	$1f_{7/2}$	0.98	-0.27	0.52	0.14	0.66	0.95	0.26	0.51	-0.13	0.38

Table 1(a) : Static IS and IV quadrupole polarizability, and static electric quadrupole polarization charge calculated for neutron and proton orbitals in $^{40}_{20}Ca_{20}$ using the SkM* interaction. The effective IV polarizability $k^{eff}_{pol}(IV)$ is defined in eq.(20). The polarization charges, e^{IS}_{pol} , $\tau_z e^{IV}_{pol}$, e^{n}_{pol} and e^{p}_{pol} , are expressed in units of e . The HF single-particle wave functions are used for the states $|i>$ and $|f>$. See the text for details.

$^{60}_{20}Ca_{40}$		neutrons					protons				
f	i	χ^{IS}_{pol}	$k^{eff}_{pol}(IV)$	e^{IS}_{pol}	$\tau_z\, e^{IV}_{pol}$	e^{n}_{pol}	χ^{IS}_{pol}	$k^{eff}_{pol}(IV)$	e^{IS}_{pol}	$\tau_z\, e^{IV}_{pol}$	e^{p}_{pol}
$1d_{5/2}$	$1d_{5/2}$						0.89	0.26	0.28	-0.12	0.17
$1d_{3/2}$	$1d_{3/2}$						0.89	0.26	0.28	-0.11	0.16
$1f_{7/2}$	$1f_{7/2}$						1.00	0.27	0.30	-0.11	0.19
$1f_{5/2}$	$1f_{5/2}$	0.73	-0.18	0.25	0.08	0.33					
$1g_{9/2}$	$1g_{9/2}$	0.75	-0.16	0.26	0.07	0.33					

Table 1(b) : Static IS and IV quadrupole polarizability, and static electric quadrupole polarization charge calculated for neutron and proton orbitals in $^{60}_{20}Ca_{40}$ using the SkM* interaction. See the caption to table 1(a).

$^{34}_{20}Ca_{14}$		neutrons					protons				
f	i	χ^{IS}_{pol}	$k^{eff}_{pol}(IV)$	e^{IS}_{pol}	$\tau_z\, e^{IV}_{pol}$	e^{n}_{pol}	χ^{IS}_{pol}	$k^{eff}_{pol}(IV)$	e^{IS}_{pol}	$\tau_z\, e^{IV}_{pol}$	e^{p}_{pol}
$1d_{5/2}$	$1d_{5/2}$	1.82 (0.99)	0.02 (-0.33)	0.96 (0.56)	0.10 (0.19)	1.06 (0.75)	1.99 (0.75)	0.71 (0.18)	0.92 (0.54)	-0.11 (-0.19)	0.81 (0.35)
$1d_{3/2}$	$1d_{3/2}$	1.75 (0.97)	0.02 (-0.32)	0.91 (0.54)	0.11 (0.19)	1.02 (0.73)	1.66 (0.65)	0.58 (0.15)	0.80 (0.48)	-0.11 (-0.17)	0.69 (0.31)

Table 1(c) : Static IS and IV quadrupole polarizability, and static electric quadrupole polarization charge calculated for neutron and proton orbitals in $^{34}_{20}Ca_{14}$ using the SkM* interaction. Inside of the parentheses we show the polarizabilities estimated by excluding the contributions from the two very sharp peaks at 3.17 and 7.56 MeV. See the caption to table 1(a).

$^{48}_{28}Ni_{20}$		neutrons					protons				
f	i	χ^{IS}_{pol}	$k^{eff}_{pol}(IV)$	e^{IS}_{pol}	$\tau_z\, e^{IV}_{pol}$	e^{n}_{pol}	χ^{IS}_{pol}	$k^{eff}_{pol}(IV)$	e^{IS}_{pol}	$\tau_z\, e^{IV}_{pol}$	e^{p}_{pol}
$1d_{3/2}$	$1d_{3/2}$	1.83 (0.85)	-0.73 (-0.36)	1.16 (0.53)	0.27 (0.15)	1.43 (0.68)					
$1f_{7/2}$	$1f_{7/2}$	2.11 (0.94)	-0.81 (-0.37)	1.28 (0.58)	0.35 (0.16)	1.63 (0.74)	1.42 (0.79)	-0.10 (0.14)	1.20 (0.54)	-0.33 (-0.15)	0.88 (0.39)

Table 2(a) : Static IS and IV quadrupole polarizability, and static electric quadrupole polarization charge calculated for neutron and proton orbitals in $^{48}_{28}Ni_{20}$ using the SkM* interaction. The effective IV polarizability $k^{eff}_{pol}(IV)$ is defined in eq.(20). The polarization charges are expressed in units of e . Inside of the parentheses we show the polarizabilities estimated by excluding the contributions from the two very sharp peaks at 3.02 and 8.03 MeV. The HF single-particle wave functions are used for the states $|i>$ and $|f>$. See the text for details.

$^{48}_{20}Ca_{28}$		neutrons					protons				
f	i	χ^{IS}_{pol}	$k^{eff}_{pol}(IV)$	e^{IS}_{pol}	$\tau_z\, e^{IV}_{pol}$	e^{n}_{pol}	χ^{IS}_{pol}	$k^{eff}_{pol}(IV)$	e^{IS}_{pol}	$\tau_z\, e^{IV}_{pol}$	e^{p}_{pol}
$1d_{3/2}$	$1d_{3/2}$						1.85 (0.82)	0.62 (0.29)	0.53 (0.32)	-0.07 (-0.12)	0.46 (0.20)
$1f_{7/2}$	$1f_{7/2}$	1.45 (0.81)	-0.01 (-0.21)	0.57 (0.33)	0.04 (0.11)	0.61 (0.44)	2.10 (0.91)	0.68 (0.29)	0.58 (0.34)	-0.04 (-0.11)	0.54 (0.23)
$2p_{3/2}$	$2p_{3/2}$	1.13 (0.60)	0.01 (-0.15)	0.42 (0.25)	0.04 (0.08)	0.46 (0.33)					

Table 2(b) : Static IS and IV quadrupole polarizability, and static electric quadrupole polarization charge calculated for neutron and proton orbitals in $^{48}_{20}Ca_{28}$ using the SkM* interaction. Inside of the parentheses we show the polarizabilities estimated by excluding the contributions from the two excited states at 3.59 and 9.00 MeV, which lie below the threshold. See the caption to table 2(a).

$^{28}_{8}O_{20}$		neutrons					protons				
f	i	χ^{IS}_{pol}	$k^{eff}_{pol}(IV)$	e^{IS}_{pol}	$\tau_z\, e^{IV}_{pol}$	e^{n}_{pol}	χ^{IS}_{pol}	$k^{eff}_{pol}(IV)$	e^{IS}_{pol}	$\tau_z\, e^{IV}_{pol}$	e^{p}_{pol}
$1d_{5/2}$	$1d_{5/2}$	0.69	-0.18	0.22	0.07	0.29	0.88	0.16	0.25	-0.08	0.17
$1d_{3/2}$	$1d_{3/2}$	0.48	-0.10	0.15	0.04	0.19	0.88	0.17	0.23	-0.06	0.17

Table 3(a) : Static IS and IV quadrupole polarizability, and static electric quadrupole polarization charge calculated for neutron and proton orbitals in $^{28}_{8}O_{20}$ using the SkM* interaction. The effective IV polarizability $k^{eff}_{pol}(IV)$ is defined in eq.(20). The polarization charges are expressed in units of e . The HF single-particle wave functions are used for the states $|i>$ and $|f>$. See the text for details.

$^{28}_{8}O_{20}$		neutrons					protons				
f	i	χ^{IS}_{pol}	$k^{eff}_{pol}(IV)$	e^{IS}_{pol}	$\tau_z\, e^{IV}_{pol}$	e^{n}_{pol}	χ^{IS}_{pol}	$k^{eff}_{pol}(IV)$	e^{IS}_{pol}	$\tau_z\, e^{IV}_{pol}$	e^{p}_{pol}
$1d_{5/2}$	$1d_{5/2}$	0.62	-0.26	0.22	0.09	0.31	0.69	0.09	0.26	-0.10	0.15
$1d_{3/2}$	$1d_{3/2}$	0.41	-0.15	0.14	0.05	0.19	0.70	0.10	0.24	-0.09	0.15

Table 3(b) : Static IS and IV quadrupole polarizability, and static electric quadrupole polarization charge calculated for neutron and proton orbitals in $^{28}_{8}O_{20}$ using the SIII interaction. See the caption to table 3(a).

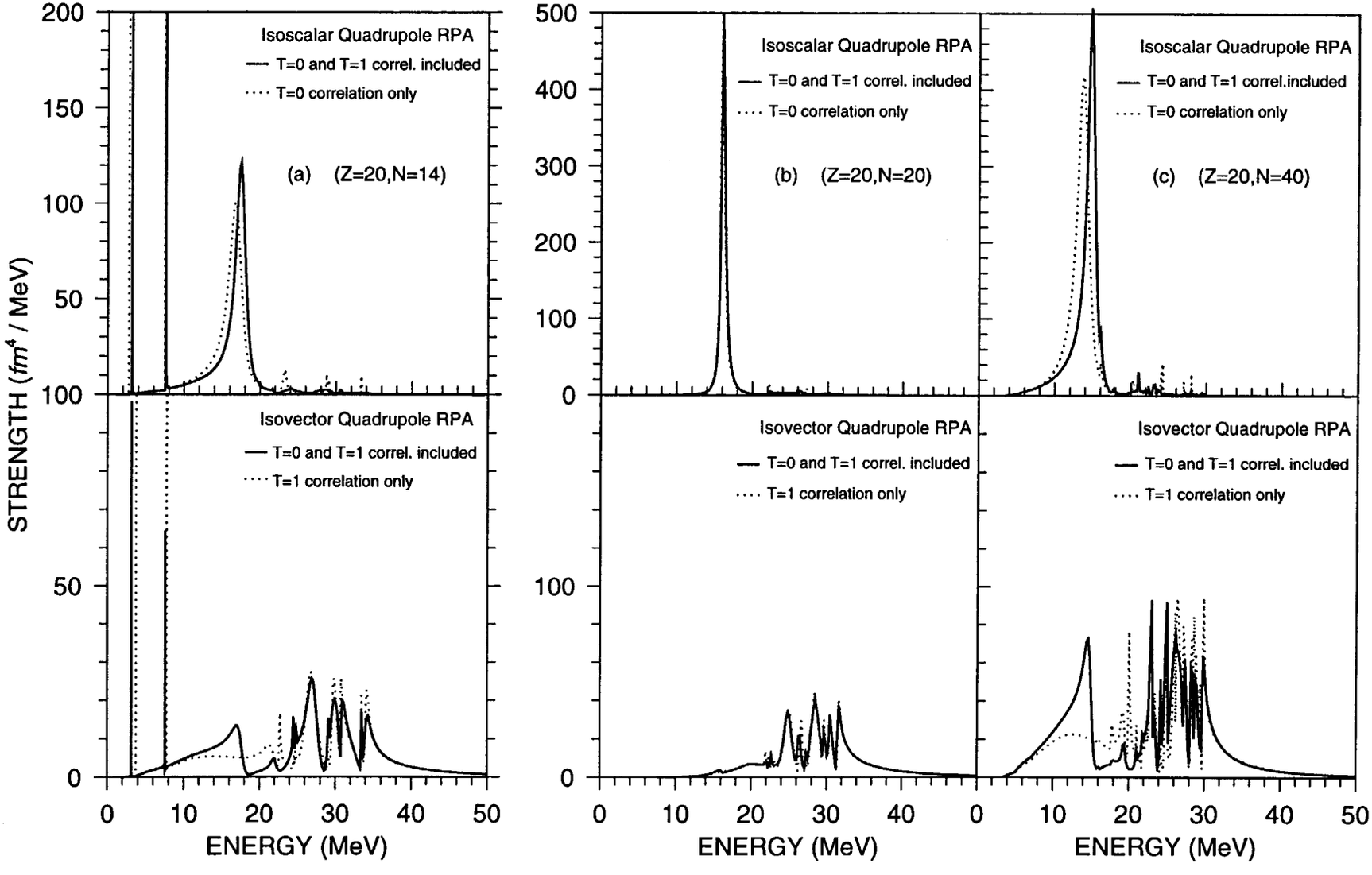
Isoscalar Quadrupole RPA
T=0 and T=1 correl. included
T=0 correlation only
(a) (Z=20,N=14)
(b) (Z=20,N=20)
(c) (Z=20,N=40)
Isovector Quadrupole RPA
T=0 and T=1 correl. included
T=1 correlation only
STRENGTH (fm⁴ / MeV)
ENERGY (MeV)

Fig. 1

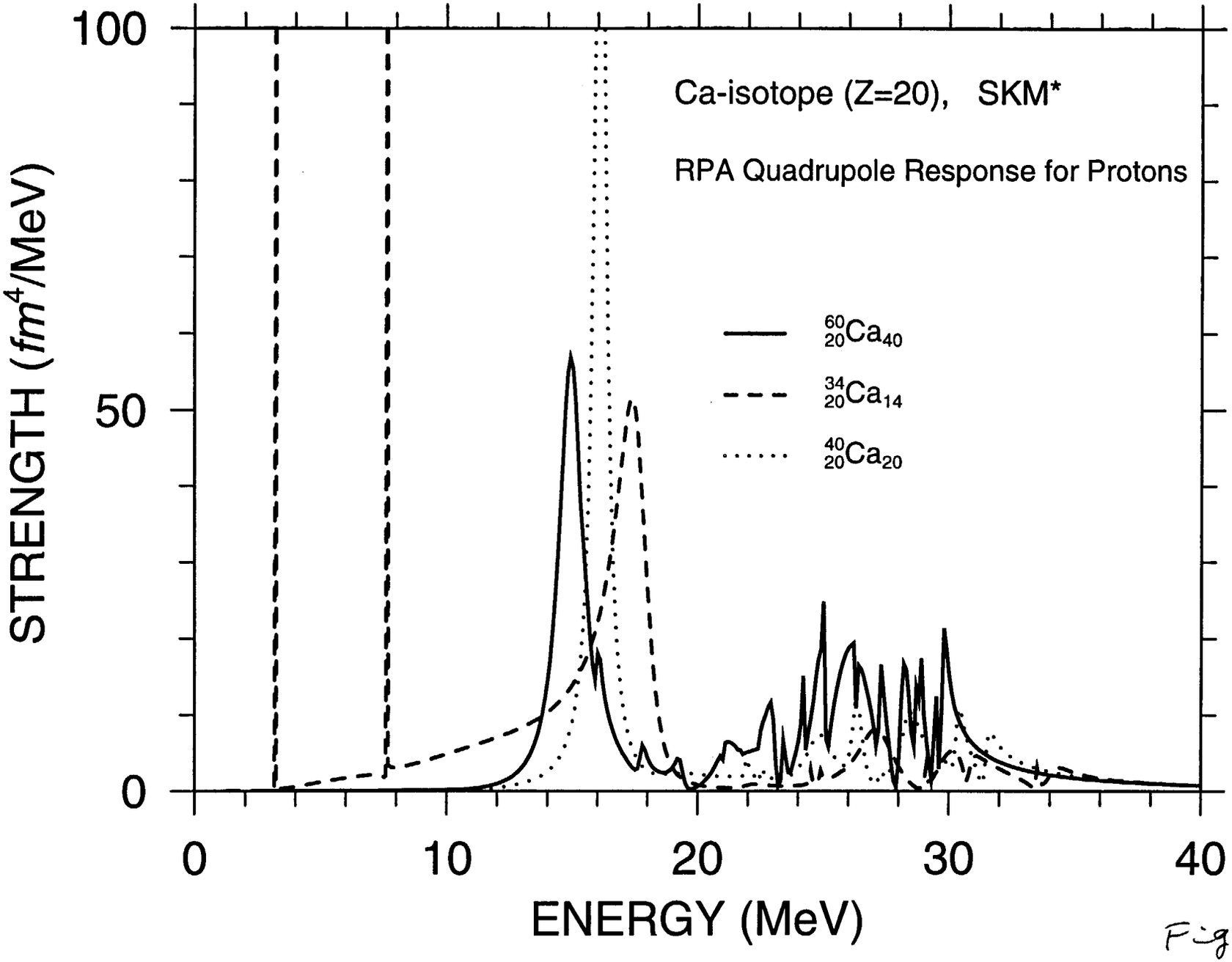
100
50
0
STRENGTH (fm^4/MeV)
Ca-isotope (Z=20), SKM*
RPA Quadrupole Response for Protons
$^{60}_{20}Ca_{40}$
$^{34}_{20}Ca_{14}$
$^{40}_{20}Ca_{20}$
0
10
20
30
40
ENERGY (MeV)

Fig. 2

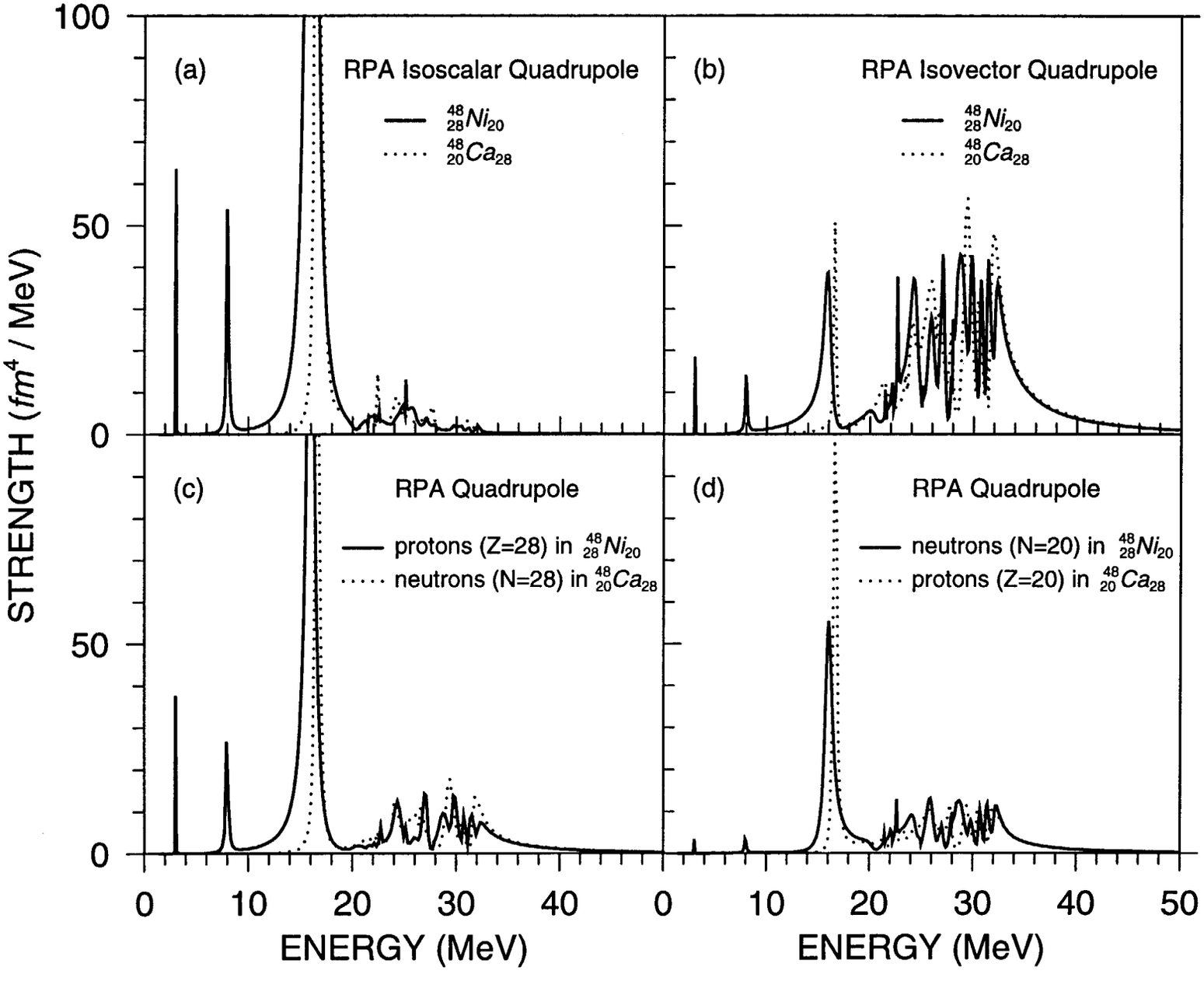
100
50
0
(a)
RPA Isoscalar Quadrupole
$^{48}_{28}Ni_{20}$
$^{48}_{20}Ca_{28}$
(b)
RPA Isovector Quadrupole
$^{48}_{28}Ni_{20}$
$^{48}_{20}Ca_{28}$
(c)
RPA Quadrupole
protons (Z=28) in $^{48}_{28}Ni_{20}$
neutrons (N=28) in $^{48}_{20}Ca_{28}$
(d)
RPA Quadrupole
neutrons (N=20) in $^{48}_{28}Ni_{20}$
protons (Z=20) in $^{48}_{20}Ca_{28}$
STRENGTH (fm^4 / MeV)
0
10
20
30
40
50
ENERGY (MeV)
ENERGY (MeV)

Fig. 3

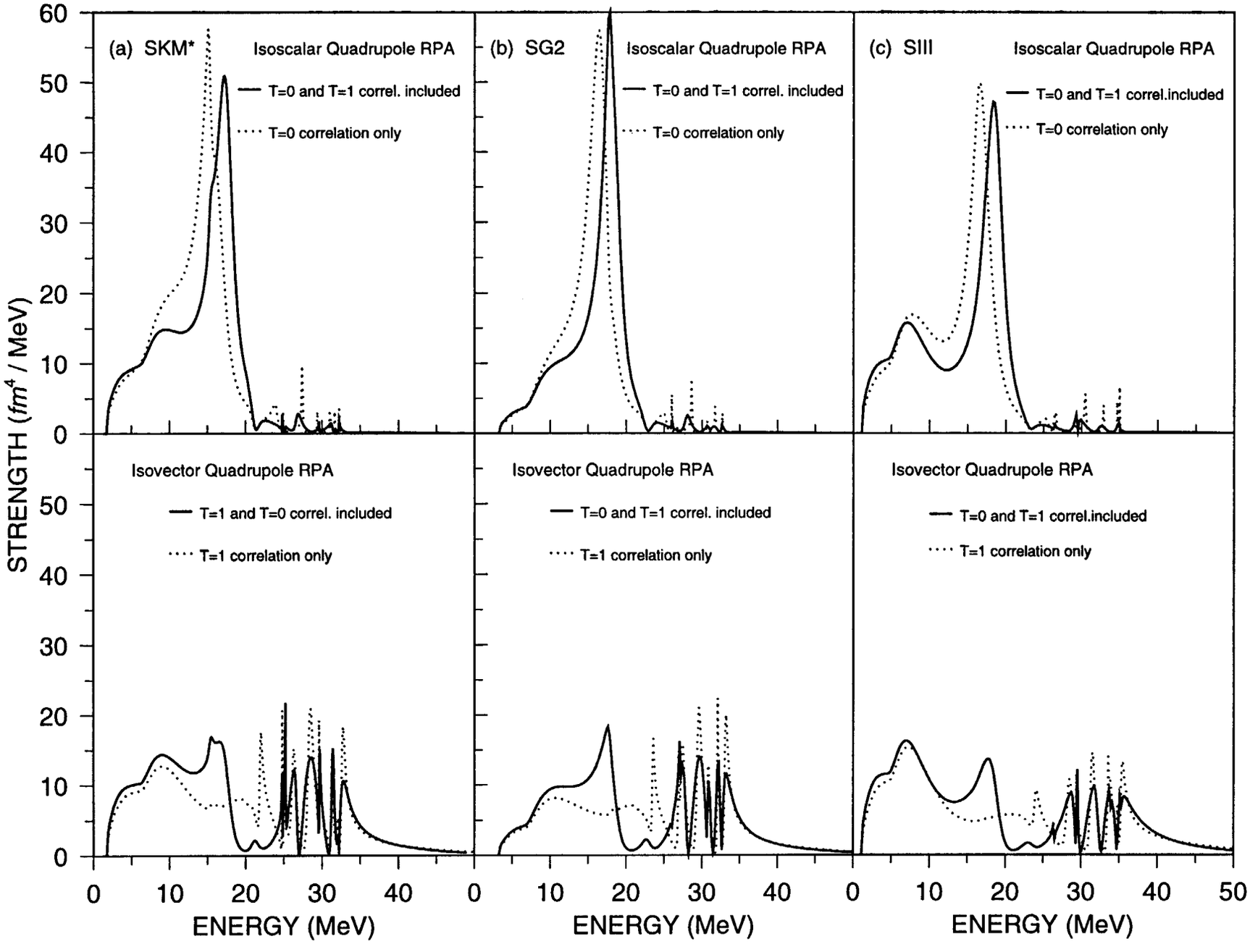
(a) SKM*
Isoscalar Quadrupole RPA
T=0 and T=1 correl. included
T=0 correlation only
(b) SG2
Isoscalar Quadrupole RPA
T=0 and T=1 correl. included
T=0 correlation only
(c) SIII
Isoscalar Quadrupole RPA
T=0 and T=1 correl.included
T=0 correlation only
Isovector Quadrupole RPA
T=1 and T=0 correl. included
T=1 correlation only
Isovector Quadrupole RPA
T=0 and T=1 correl. included
T=1 correlation only
Isovector Quadrupole RPA
T=0 and T=1 correl.included
T=1 correlation only
STRENGTH (fm⁴ / MeV)
ENERGY (MeV)
ENERGY (MeV)
ENERGY (MeV)

Fig.4